Published in final edited form as:
Nature. 2011 May 12; 473(7346): 221–225. doi:10.1038/nature09915.

Modeling schizophrenia using hiPSC neurons

Kristen Brennand[1], **Anthony Simone**[1,*], **Jessica Jou**[1,*], **Chelsea Gelboin-Burkhart**[1,*], **Ngoc Tran**[1,*], **Sarah Sangar**[1], **Yan Li**[1], **Yangling Mu**[1], **Gong Chen**[2], **Diana Yu**[1], **Shane McCarthy**[3], **Jonathan Sebat**[4], and **Fred H. Gage**[1]

[1]Salk Institute for Biological Studies, Laboratory of Genetics, 10010 North Torrey Pines Road, La Jolla CA 92037

[2]Department of Biology, Pennsylvania State University, 201 Life Science Building, University Park, PA 16802

[3]Cold Spring Harbor Laboratory, 1 Bungtown Rd., Cold Spring Harbor, NY 11724

[4]University of California San Diego, Department of Psychiatry and Department of Cellular and Molecular Medicine, University Of California, San Diego, La Jolla, CA 92093

SUMMARY

Schizophrenia (SCZD) is a debilitating neurological disorder with a world-wide prevalence of 1%; there is a strong genetic component, with an estimated heritability of 80–85%[1]. Though postmortem studies have revealed reduced brain volume, cell size, spine density and abnormal neural distribution in the prefrontal cortex and hippocampus of SCZD brain tissue[2] and neuropharmacological studies have implicated dopaminergic, glutamatergic and GABAergic activity in SCZD[3], the cell types affected in SCZD and the molecular mechanisms underlying the disease state remain unclear. To elucidate the cellular and molecular defects of SCZD, we directly reprogrammed fibroblasts from SCZD patients into human induced pluripotent stem cells (hiPSCs) and subsequently differentiated these disorder-specific hiPSCs into neurons (SI Fig. 1). SCZD hiPSC neurons showed diminished neuronal connectivity in conjunction with decreased neurite number, PSD95-protein levels and glutamate receptor expression. Gene expression profiles of SCZD hiPSC neurons identified altered expression of many components of the cAMP and WNT signaling pathways. Key cellular and molecular elements of the SCZD phenotype were ameliorated following treatment of SCZD hiPSC neurons with the antipsychotic Loxapine. To date, hiPSC neuronal pathology has only been demonstrated in diseases characterized by both the loss of function of a single gene product and rapid disease progression in early childhood[4–6]. We now report hiPSC neuronal phenotypes and gene expression changes associated with SCZD, a complex genetic psychiatric disorder (SI Table 1).

CONTACT: Fred H. Gage, gage@salk.edu, phone 858.453.4100, fax 858.597.0824.
*These authors contributed equally to this work.

SI Information is linked to the online version of the paper at www.nature.com/nature.

AUTHOR CONTRIBUTIONS

K.J.B. designed the experiments with F.G. K.J.B. completed the experiments and wrote the manuscript. A.S. contributed to the microarray analysis and qPCR experiments. J.J. established the synaptic density assay and completed the calcium transient experiments. C.G.B. and S.S. performed most of the synaptic protein experiments. NT analyzed the rabies data. N.T. and S.S. together counted neurites. Y.L., Y.M. and G.C. performed electrophysiology. D.Y. established the calcium transient assay. S.M.C. and J.S. completed the CNV analysis.

AUTHOR INFORMATION

The data discussed in this publication have been deposited in NCBI's Gene Expression Omnibus (Brennand et al., 2010) and are accessible through GEO Series accession number GSE25673 (http://www.ncbi.nlm.nih.gov/geo/query/acc.cgi?acc=GSE25673). As per our agreement with Coriell Cell Repository, all hiPSC lines generated from control and schizophrenic fibroblasts will only be available from Coriell.

The authors have declared that no competing interests exist.

RESULTS

Four SCZD patients were selected: patient 1, diagnosed at six years of age, had childhood-onset SCZD; patients 2, 3 and 4 were from families in which all offspring and one parent were affected with psychiatric disease (SI Fig. 3A). Primary human fibroblasts (HFs) were reprogrammed using inducible lentiviruses[7]. Control and SCZD hiPSCs expressed endogenous pluripotency genes, repressed viral genes and were indistinguishable in assays for self-renewal and pluripotency (Fig. 1; SI Fig. 2). SCZD hiPSCs had no apparent defects in generating neural progenitor cells (NPCs) or neurons (Fig. 1; SI Fig. 3). Most hiPSC neurons were presumably glutamatergic and expressed VGLUT1 (SI Fig. 8A). Approximately 30% of neurons were GAD67-positive (GABAergic) (SI Fig. 8C,D) whereas less than 10% of neurons were tyrosine hydroxylase (TH)-positive (dopaminergic) (SI Fig. 7).

Neuronal connectivity was assayed using trans-neuronal spread of rabies; *in vivo*, rabies transmission occurs via synaptic contacts and is strongly correlated with synaptic input strength[8]. Primary infection was restricted by replacing the rabies coat protein with envelope A (ENVA), which infects only via the avian tumor virus A (TVA) receptor; viral spread was limited to monosynaptically connected neurons by deleting the rabies glycoprotein gene (ΔG)[9]. Neurons were first transduced with a lentivirus expressing Histone 2B (H2B)-green fluorescent protein (GFP) fusion protein, TVA and G from the synapsin (SYN) promoter (LV-SYNP-HTG). One week later, neurons were transduced with modified rabies (Rabies-ENVAΔG-RFP). Primary infected cells were positive for both H2BGFP and RFP; neurons monosynaptically connected to primary cells were GFP-negative but RFP-positive (SI Fig. 4A). Transduction with Rabies-ENVAΔG-RFP alone resulted in no RFP-positive cells, whereas transduction with Rabies-ENVAΔG-RFP following lentiviral transduction without rabies glycoprotein (SYNP-HT) led to only single GFP^+RFP^+ cells, indicating that *in vitro* rabies infection and spread are dependent on TVA expression and G trans-complementation, respectively (SI Fig. 4C,D).

There was decreased neuronal connectivity in SCZD hiPSC neurons (Fig. 2; SI Fig. 4B,C; SI Fig. 5,6). FACS analysis confirmed differences in neuronal connectivity and demonstrated that comparable numbers of βIII-tubulin-positive neurons were labeled with LV-SYNP-HTG. Though the mechanism of rabies trans-neuronal tracing is not fully understood, the presynaptic protein NCAM has been implicated[10]; NCAM expression is decreased in SCZD hiPSC neurons (SI Table 3). Rabies trans-neuronal tracing occurs in functionally immature hiPSC neurons (SI Fig. 4E) and in the presence of the voltage-gated sodium channel blocker tetrodotoxin (TTX) (1μM), depolarizing KCl (50mM) or the calcium channel blocker ryanodine (10μM) (SI Fig. 4F). Decreased trans-neuronal tracing is evidence of decreased neuronal connectivity, but not necessarily decreased synaptic function, in SCZD hiPSC neurons.

We tested the ability of five antipsychotic drugs to improve neuronal connectivity *in vitro*. Clozapine, Loxapine, Olanzapine, Risperidone and Thioridazine were administered for the final three weeks of neuronal differentiation. Only Loxapine significantly increased neuronal connectivity in hiPSC neurons from all patients (Fig. 2B; SI Fig. 5). Optimization of the concentration and timing of drug administration may improve the effects of the other antipsychotic medications.

Reduced dendritic arborization has been observed in postmortem SCZD brains[11] and in animal models[12]. SCZD hiPSC neurons show a decrease in the number of neurites (Fig. 3A; SI Fig. 9A,B). Synaptic genes are associated with SCZD[13] (SI Fig. 9D) and impaired

synaptic maturation occurs in a number of mouse models[12]. hiPSC neurons express dense puncta of synaptic markers that co-stain for both pre- and post-synaptic markers (SI Fig. 8A,B). While we observed decreased PSD95 protein expression relative to MAP2AB in SCZD hiPSC neurons (Fig. 3B; SI Fig. 9H), the levels of SYN, VGLUT1, GLUR1, VGAT and GEPH were unaffected (SI Fig. 9E–J). Decreased PSD95 synaptic density in SCZD hiPSC neurons failed to reach statistical significance (Fig. 3C; SI Fig. 9C).

We used electrophysiology and calcium transient imaging to measure spontaneous neuronal activity (Fig. 3D–K; SI Fig. 10). SCZD hiPSC neurons showed normal transient inward sodium currents and sustained outward potassium currents in response to membrane depolarizations (Fig. 3D), action potentials to somatic current injections, (Fig. 3E), excitatory postsynaptic currents (EPSCs) (Fig. 3F) and inhibitory postsynaptic currents (IPSCs) (Fig. 3G). The amplitude and rate of spontaneous calcium transients were unaffected (Fig. 3H–J; SI Fig. 10A–D) and there was no difference in synchronicity of spontaneous calcium transients (Fig. 3K; SI Fig. 10E–G).

Increased NRG1 expression has been observed in postmortem SCZD brain tissue[13]. NRG1 expression was increased in SCZD hiPSC neurons (Fig. 4D–F) but not SCZD fibroblasts (HF), hiPSCs or NPCs (Fig. 4E), demonstrating the importance of studying gene expression changes in the cell type relevant to disease. In all, 596 unique genes (271 upregulated and 325 downregulated) showed greater than 1.30-fold-expression changes between SCZD and control hiPSC neurons ($p<0.05$) (SI Fig. 11A,B; SI Table 3). Of these genes, 13% (74) have published associations with SCZD and 16% (96) have been linked to SCZD by postmortem gene expression profiles available through the Stanley Medical Research Institute[14] (SI Table 3); in total 25% (149) of our differentially expressed genes have been previously implicated in SCZD. Gene ontology (GO) analysis identified significant perturbations of glutamate, cAMP and WNT signaling (Fig. 4A–C; SI Table 4; SI Fig. 11C), pathways required for activity-dependent refinement of synaptic connections and long-term potentiation[15–17]. Sixteen of 17 candidate genes from these families were validated by qPCR (SI Table 2; Fig. 4F; SI Fig. 11E).

Copy number variants (CNVs) are rare, highly penetrant structural disruptions. SCZD patients have a 1.15-fold increase in CNV burden, but how this translates into illness is unknown. Patient 4 had four CNVs involving genes previously associated with SCZD or bipolar disorder (BD)[13,18,19]; of these, neuronal expression of NRG3 and GALNT11, but not of CYP2C19 or GABARB2/GABARA6 was affected (SI Fig. 12, SI Table 5). A second analysis of CNVs unbiased by previous GWAS studies identified 42 genes affected by CNVs in our four SCZD patients (SI Table 5). Though twelve of these genes showed altered neuronal expression consistent with genotype ($p<0.05$), most changes were extremely small and only three (CSMD1, MYH1, MYH4) showed >1.3-fold effects (SI Table 5). Well-established SCZD CNVs occur at 1q21.1, 15q11.2, 15q13.3, 16p11.2 and 22q11.2,[13,18,19], but the relevant genes remain unidentified. Our patients had no evidence of CNVs at these regions, and gene expression of the best candidate genes in each region, such as GJA8 (1q21.1), CYFIP1 (15q11.1), CHRFAM7A (15q13.3), PRODH (22q11.2), COMT (22q11.2) and ZDHHC8 (22q11.2)[18,20], was not affected in our SCZD hiPSC neurons (SI Table 6).

Consistent with published reports, Loxapine increased NRG1 expression in neurons[21]. Loxapine also increased expression of several glutamate receptors. ADCY8, PRKCA, WNT7A and TCF4 also showed ameliorated expression with Loxapine (Fig. 4F; SI Fig. 11E).

DISCUSSION

SCZD hiPSC neurons from heterogeneous patients had similar deficits, replicating some but not all aspects of the cellular and molecular phenotypes observed in post-mortem human studies and animal models (SI Table 1). We observed decreased neuronal connectivity in SCZD hiPSC neurons, but not defects in synaptic function; this may reflect technical limitations of our synaptic activity assays. Due to the heterogeneity of our patient cohort and small sample size, our findings might not generalize to all subtypes of SCZD and our microarray comparisons of SCZD and control hiPSC neurons are necessarily preliminary. Gene expression studies of hiPSC neurons permit straightforward comparisons of antipsychotic treatments on live, genetically identical neurons from patients with known clinical treatment outcomes, eliminating many confounding variables of postmortem analysis such as treatment history, drug or alcohol abuse, and cause of death. For example, though Loxapine is characterized as a high affinity antagonist of serotonin 5-HT_2 receptors and dopamine D_1, D_2 and D_4 receptors[22], treatment of SCZD hiPSC neurons resulted in altered gene expression and increased neuronal connectivity.

Of the 596 unique genes differentially expressed in our SCZD hiPSC neurons (>1.30-fold, $p<0.05$), 25% have been previously implicated in SCZD (SI Table 3). While our gene expression profiles of SCZD hiPSC neurons confirm and extend the major hypotheses generated by pharmacological and GWAS studies of SCZD, they also identify some pathways not before linked to SCZD, such as NOTCH signaling, SLIT/ROBO axon guidance, EFNA mediated axon growth, cell adhesion and transcriptional silencing (SI Table 4). Many of the genes most affected in SCZD hiPSC neurons belong to pathways previously associated with SCZD, though they have not yet been singled out as SCZD genes. For example, while PDE4B is a well-characterized SCZD gene, we observed significant misexpression of PDE1C, PDE3A, PDE4D, PDE4DIP, PDE7B, ADCY7 and ADCY8. Additionally, though some key SCZD/BD genes, including NRG1 and ANK3, were misexpressed in all of our SCZD hiPSC neurons, many others, including ZNF804A, GABRB1, ERBB4, DISC1 and PDE4B, were aberrantly expressed in some but not all patients. Our data support the "watershed model"[23] of SCZD whereby many different combinations of gene misfunction may disrupt the key pathways affected in SCZD. We predict that, as the number of SCZD cases studied using hiPSC neurons increases, a diminishing number of genes will be consistently affected across the growing patient cohort; instead, evidence will accumulate that a handful of essential pathways can be disrupted in diverse ways to result in SCZD.

METHODS SUMMARY

Reprogramming hiPSCs

Control and SCZD HFs were obtained from cell repositories and were reprogrammed with tetracycline-inducible lentiviruses expressing the transcription factors OCT4, SOX2, KLF4, cMYC and LIN28[7]. Lentiviruses were packaged in 293T HEK cells transfected with Polyethylenimine (PEI) (Polysciences). HFs were transduced and then split onto mouse embryonic fibroblasts (mEFs). Cells were switched to HUES media (KO-DMEM (Invitrogen), 10% KO-Serum Replacement (Invitrogen), 10% Plasminate (Talecris), 1x Glutamax (Invitrogen), 1x NEAA (Invitrogen), 1x 2 mercaptoethanol (Sigma) and 20 ng/ml FGF2 (Invitrogen)) and 1 μg/ml Doxycycline (Sigma) was added to HUES media for the first 21–28 days of reprogramming. hiPSCs were generally grown in HUES media: early passage hiPSCs were split through manual passaging, while at higher passages hiPSCs could be enzymatically passaged with 1mg/ml Collagenase (Sigma).

hiPSC differentiation to NPCs and neurons

Embryoid bodies were generated from hiPSCs and then transferred to nonadherent plates (Corning). Colonies were maintained in suspension in N2 media (DMEM/F12 (Invitrogen), 1x N2 (Invitrogen)) for 7 days and then plated onto polyornithine (PORN)/Laminin-coated plates. Visible rosettes formed within 1 week and were manually dissected and cultured in NPC media (DMEM/F12, 1x N2, 1x B27-RA (Invitrogen), 1 μg/ml Laminin (Invitrogen) and 20 ng/ml FGF2 (Invitrogen). NPCs are maintained at high density, grown on PORN/Laminin-coated plates in NPC media and split approximately 1:4 every week with Accutase (Millipore). For neural differentiations, NPCs were dissociated with Accutase and plated at low density in neural differentiation media (DMEM/F12-Glutamax, 1x N2, 1x B27-RA, 20 ng/ml BDNF (Peprotech), 20 ng/ml GDNF (Peprotech), 1 mm dibutyrl-cyclicAMP (Sigma), 200 nM ascorbic acid (Sigma) onto PORN/Laminin-coated plates.

Assays for neuronal connectivity, neurite outgrowth, synaptic protein expression, synaptic density, electrophysiology, spontaneous calcium transient imaging and gene expression were used to compare control and SCZD hiPSC neurons.

Additional methods are found in S.I.

METHODS

Description of SCZD patients

All patient samples were obtained from the Coriell collection. Patients were selected based on the high likelihood of a genetic component to disease. Patient 1 (GM02038, male, 22 years of age, Caucasian) was diagnosed with SCZD at six years of age and committed suicide at 22 years of age. Patient 2 (GM01792, male, 26 years of age, Jewish Caucasian) displayed episodes of agitation, delusions of persecution, and fear of assassination. His sister, patient 3 (GM01835, female, 27 years of age, Jewish Caucasian) had a history of schizoaffective disorder and drug abuse. Patient 4 (GM02497, male, 23 years of age, Jewish Caucasian) was diagnosed with SCZD at age 15 and showed symptoms including paralogical thinking, affective shielding, splitting of affect from content, and suspiciousness. His sister, patient 5 (GM02503, female, 27 years of age, Jewish Caucasian) was diagnosed with anorexia nervosa in adolescence and with schizoid personality disorder (SPD) as an adult. SPD has an increased prevalence in families with SCZD but is a milder diagnosis characterized not by psychosis but rather by a lack of interest in social relationships and emotional coldness[24]. Though we show data from SPD patient 5 as an interesting point of comparison, we do not consider patient 5 to belong to either the “control” or “SCZD” groups.

Preliminary experiments were controlled using BJ fibroblasts from ATCC (CRL-2522). These fibroblasts were expanded from foreskin tissue of a newborn male. They are readily reprogrammed, low passage, karyotypically normal and extremely well-characterized primary fibroblast line cells. Age and ancestry matched controls were obtained from three Coriell collections: apparently healthy individuals with normal psychiatric evaluations, apparently healthy non-fetal tissue and gerontology research center cell cultures. hiPSCs were generated from GM02937 (male, 22 years of age), and GM03440 (male, 20 years of age), GM03651 (female, 25 years of age), GM04506 (female, 22 years of age), AG09319 (female, 24 years of age) and AG09429 (female, 25 years of age).

Generation of lentivirus

Lentivirus was packaged in 293T HEK cells grown in 293T media (IMEM (Invitrogen), 10% FBS (Gemini), 1xGlutamax(Invitrogen)). 293T cells were transfected with

Polyethylenimine (PEI) (Polysciences). Per 15-cm plate, the following solution was prepared, incubated for 5 minutes at room temperature and added drop-wise to plates: 12.2 μg lentiviral DNA, 8.1 μg MDL-gagpol, 3.1 μg Rev-RSV, 4.1 μg CMV-VSVG, 500 μl of IMDM and 110 μl PEI (1 μg/μl) and vortexed lightly. Medium was changed after three hours and the virus was harvested at 48 and 72 hours post transfection.

hiPSC derivation

HFs were cultured on plates treated with 0.1% gelatin (in milli Q water) for a minimum of 30 minutes and grown in HF media (DMEM (Invitrogen), 10% FBS (Gemini), 1x Glutamax (Invitrogen), 5 ng/ml FGF2 (Invitrogen)).

HFs were infected daily for five days with tetracycline-inducible lentiviruses expressing OCT4, SOX2, KLF4, cMYC and LIN28, driven by a sixth lentivirus expressing the reverse tetracycline transactivator (rtTA)[7]. Cells from a single well of a six-well dish were split onto a 10-cm plate containing 1 million mouse embryonic fibroblasts (mEFs). Cells were switched to HUES media (KO-DMEM (Invitrogen), 10% KO-Serum Replacement (Invitrogen), 10% Plasminate (Talecris), 1x Glutamax (Invitrogen), 1x NEAA (Invitrogen), 1x 2 mercaptoethanol (Sigma) and 20 ng/ml FGF2 (Invitrogen)). 1 μg/ml Doxycycline (Sigma) was added to HUES media at for the first 21–28 days of reprogramming.

hiPSC colonies were manually picked and clonally plated onto 24-well mEF plates. hiPSC lines were either maintained on mEFs in HUES media or on Matrigel (BD) in TeSR media (Stemcell Technologies). At early passages, hiPSCs were split through manual passaging. At higher passages, hiPSC could be enzymatically passaged with Collagenase (1mg/ml in DMEM) (Sigma). Cells were frozen in freezing media (DMEM, 10% FBS, 10% DMSO).

Karyotyping analysis was performed by Cell Line Genetics (Wisconsin, MD) or by Dr. Marie Dell'Aquila (UCSD).

Teratoma analysis was performed by injecting hiPSCs into the kidney capsules of isoflorane-anesthetized NOD-SCID mice. Teratomas were harvested eight weeks post-injection, paraffin-embedded and H&E stained.

hiPSC differentiation to NPCs and neurons

hiPSCs grown in HUES media on mEFs were incubated with Collagenase (1 mg/ml in DMEM) at 37°C for one to two hours until colonies lifted from the plate and were transferred to a nonadherent plate (Corning). Embryoid Bodies (EBs) were grown in suspension in N2 media (DMEM/F12-Glutamax (Invitrogen), 1x N2(Invitrogen)). After seven days, EBs were plated in N2 media with 1 μg/ml Laminin (Invitrogen) onto polyornithine (PORN)/Laminin-coated plates. Visible rosettes formed within one week and were manually dissected onto PORN/Laminin-coated plates. Rosettes were cultured in NPC media (DMEM/F12, 1x N2, 1x B27-RA (Invitrogen), 1 μg/ml Laminin and 20 ng/ml FGF2) and dissociated in TrypLE (Invitrogen) for three minutes at 37°C. NPCs are maintained at high density, grown on PORN/Laminin-coated plates in NPC media and split approximately 1:4 every week with Accutase (Millipore).

For neural differentiations, NPCs were dissociated with Accutase and plated in neural differentiation media (DMEM/F12, 1x N2, 1X B27-RA, 20 ng/ml BDNF (Peprotech), 20 ng/ml GDNF (Peprotech), 1 mm dibutyrl-cyclicAMP (Sigma), 200 nm ascorbic acid (Sigma) onto PORN/Laminin-coated plates. Density is critical and the following guidelines were used: two-well permanox slide, 80–100,000 cells/well; 24-well, 40–60,000 cells/well; six-well, 200,000 cells/well. hiPSC derived-neurons were differentiated for 1–3 months. Notably, synapse maturation occurs most robustly *in vitro* when hiPSC neurons are

cocultured with wildtype human cerebellar astrocytes (Sciencell). 0.5% FBS was supplemented into neural differentiation media for all astrocyte coculture experiments.

It is difficult to maintain healthy neurons for three months of differentiation and some cultures invariably fail or become contaminated. When even one SCZD patient neural culture failed, the experiments were abandoned as all assays were conducted on neurons cultured in parallel. If, however, only a control neural culture failed, and at least three control samples remained, analysis was completed. For this reason, though patients are consistently numbered throughout the manuscript, controls are not, and are instead listed in numerical order (BJ, GM02937, GM03651, GM04506, AG09319, AG09429).

Antipsychotic drugs were added for the final three weeks of a three-month differentiation on astrocytes and for the final two weeks of a six-week differentiation on PORN/laminin alone. Drugs were resuspended in DMSO at the following concentrations: Clozapine (5 μM), Loxapine (10 μM), Olanzapine (1 μM), Risperidone (10 μM) and Thioridazine (5 μM).

Immunohistochemistry

Cells were fixed in 4% paraformaldehyde in PBS at 4°C for 10 minutes. hiPSCs and NPCs were permeabilized at room temperature for 15 minutes in 1.0% Triton in PBS. All cells were blocked in 5% donkey serum with 0.1% Triton at room temperature for 30 minutes. The following primary antibodies and dilutions were used: mouse anti-Oct4 (Santa Cruz), 1:200; goat anti-Sox2 (Santa Cruz), 1:200;goat anti-Nanog (R&D), 1:200; mouse anti-Tra1-60 (Chemicon), 1:100; mouse anti-human Nestin (Chemicon), 1:200; rabbit anti-βIII-tubulin (Covance), 1:200; mouse anti-βIII-tubulin (Covance), 1:200; rabbit anti-cow-GFAP (Dako) 1:200; mouse anti-MAP2AB (Sigma), 1:200; rabbit anti-synapsin (Synaptic Systems), 1:500; mouse anti-PSD95 (UCDavis / NIH Neuromab), 1:500; rabbit anti-PSD95 (Invitrogen), 1:200 rabbit-anti-VGLUT1 (Synaptic; Systems), 1:500; rabbit anti-Gephyrin, (Synaptic Systems), 1:500; mouse anti-vGAT (Synaptic Systems), 1:500; rabbit anti-vGat (Synaptic Systems), 1:500; rabbit anti-GLUR1 (Oncogene), 1:100; rabbit anti-GABA (Sigma), 1:200; rabbit anti-GAD65/67 (Sigma), 1:200.

Secondary antibodies were Alexa donkey 488, 555 and 647 anti-rabbit (Invitrogen), Alexa donkey 488 and 555 anti-mouse (Invitrogen), and Alexa donkey 488, 555, 568 and 594 anti-goat (Invitrogen); all were used at 1:300. To visualize nuclei, slides were stained with 0.5 μg/ml DAPI (4',6-diamidino-2-phenylindole) and then mounted with Vectashield. Images were acquired using a Bio-Rad confocal microscope.

FACS

For sorting of dissociated two-month-old hiPSC neurons, cultures were dissociated in trypsin for 5 minutes, washed in DMEM, centrifuged at 500×g and resuspended in PBS. Cells were fixed in 4% paraformaldehyde in PBS at 4°C for 10 minutes. Cells were washed in PBS and aliquoted into 96-well conical plates. Cells were blocked in 5% donkey serum with 0.1% saponin at room temperature for 30 minutes. The following primary antibodies and dilutions were used for one hour at room temperature: rabbit anti-βIII-tubulin (Sigma), 1:200; mouse anti-βIII-tubulin (Covance), 1:200; rabbit anti-GAD56/67 (Sigma), 1:200. Cells were washed and then incubated with secondary antibodies at 1:200 for 30 minutes at room temperature: Alexa donkey 647 anti-rabbit (Invitrogen), and Alexa donkey 488 anti-mouse (Invitrogen). Cells were washed three times in PBS and stained with 0.5μg/ml DAPI (4',6-diamidino-2-phenylindole). Cells were resuspended in PBS with 5% donkey serum and 0.1% detergent saponin. The homogeneous solution was filtered through a 250-μM nylon sieve and run in a BD FACS Caliber. Data were analyzed using FloJo.

Rabies virus trans-neuronal tracing

Rabies virus trans-neuronal tracing was performed on three-month-old hiPSC neurons cocultured with wildtype human astrocytes (Sciencell) on acid-etched glass coverslips and then transduced with LV-SYNP-HTG or LV-SYNP-HT. Cultures were transduced with Rabies-ENVAΔG-RFP after at least a week to allow expression of ENVA and rabies G. Either 5, 7 or 10 days later, hiPSC neurons were either dissociated with accutase for FACS analysis of fixed with 4% paraformaldehyde in PBS for fluorescent microscopy.

Neurite analysis

Neurite analysis was performed on three-month-old hiPSC neurons cocultured with wildtype human astrocytes (Sciencell) on acid-etched glass. Low titer transduction of a lentivirus driving expression of GFP from the SYN promoter (LV-SYNP-GFP) occurred at least 7 days prior to assay. LV-SYNP-GFP was used to image and count branching neurites from single neurons (Fig. 3A). The number of neurites extending from the soma of 691 single LV-SYNP-GFP-labeled neurons was determined by a blinded count.

Synaptic protein staining analysis

Synaptic protein staining was performed on three-month-old hiPSC neurons cocultured with wildtype human astrocytes (Sciencell) on acid-etched glass. To calculate ratios of MAP2AB-positive dendrites and synaptic proteins, confocal images were taken at 630x magnification and 4x zoom. Using NIH ImageJ, images were thresholded and the integrated pixel density was determined for each image. Integrated pixel density measurement is the product of area (measured in square pixels) and mean gray value (the sum of the gray values of all the pixels in the selection divided by the number of pixels).

Synapse density

Synapse density analysis was performed on three-month-old hiPSC neurons cocultured with wildtype human astrocytes (Sciencell) on acid-etched glass. Manual counts of synaptic density were done in three steps using NIH ImageJ. First, the colocalization plugin was used to identify colocalization of VGLUT1 and PSD95. Second, the particle analysis function was used to restrict size 50-infinity. Third, dendrites were traced using the NeuronJ plugin. The mask generated by particle analysis was overlayed on the trace generated by NeuronJ and synapses were manually counted.

Electrophysiology

Whole-cell perforated patch recordings were performed on SCZD (n=30) and control (n=20) three-month-old hiPSC neurons cocultured with wildtype human astrocytes (Sciencell) on acid-etched coverslips and typically transduced with LV-SYNP-GFP. The recording micropipettes (tip resistance 3–6 MÙ) were tip-filled with internal solution composed of 115mM K-gluconate, 4mM NaCl, 1.5mM MgCl2, 20 mM HEPES, and 0.5mM EGTA (pH 7.4) and then back-filled with the same internal solution containing 200μg/ml amphotericinB (Calbiochem). Recordings were made using Axopatch 200B amplifier (Axon Instruments). Signals were sampled and filtered at 10kHz and 2kHz, respectively. The whole-cell capacitance was fully compensated, whereas the series resistance was uncompensated but monitored during the experiment by the amplitude of the capacitive current in response to a 5mV pulse. The bath was constantly perfused with fresh HEPES-buffered saline composed of 115mM NaCl, 2mM KCl, 10mM HEPES, 3mM $CaCl_2$, 10mM glucose and 1.5mM $MgCl_2$ (pH 7.4). For voltage-clamp recordings, cells were clamped at −60 to −80mV; Na+ currents and K+ currents were stimulated by voltage step depolarizations. Command voltage varied from −50 to +20mV in 10mV increments. For current-clamp recordings, induced

action potentials were stimulated with current steps from −0.2 to + 0.5nA. All recordings were performed at room temperature.

Spontaneous calcium transients

Calcium imaging analysis was performed on 2.5- to 3-month-old hiPSC neurons cocultured with wildtype human astrocytes (Sciencell) on acid-etched glass. Culture medium was removed and hiPSC cultures were incubated with 0.4 μM Fluo-4AM (Molecular Probes) and 0.02% Pluronic F-127 detergent in Krebs Hepes Buffer (KHB) (10 mM HEPES, 4.2 mM $NaHCO_3$, 10 mM dextrose, 1.18 mM $MgSO_4 \cdot 2H_2O$, 1.18 mM KH_2PO_4, 4.69 mM KCl, 118 mM NaCl, 1.29 mM $CaCl_2$; pH 7.3) for one hour at room temperature. Cells were washed with KHB buffer, incubated for two minutes with Hoechst dye diluted 1:1000 in KHB, and allowed to incubate for an additional 15 minutes in KHB to equilibrate intracellular dye concentration. Time-lapse image sequences (100x magnification) were acquired at 28 Hz using a Hamamatsu ORCA-ER digital camera with a 488 nm (FITC) filter on an Olympus IZ81 inverted fluorescence confocal microscope. Images were acquired with MetaMorph.

In total, eight independent neural differentiations were tested per patient, 210 movies of spontaneous calcium transients (110 control and 100 SCZD) were generated and 2,676 ROIs (1,158 control and 1,518 SCZD ROIs) were analyzed. Up to four 90-second videos of Fluo-4AM fluorescence were recorded per neural differentiation per patient with a spinning disc confocal microscope at 28 frames per second (SI Fig. 5A). Using ImageJ software, regions of interest (ROIs) can be manually selected and the mean pixel intensity of each ROI can be followed over time, generating time trace data for each ROI. The data were analyzed in Matlab where background subtraction was performed by normalizing traces among traces of the sample, and spike events were identified based on the slope and amplitude of the time trace.

The amplitude of spontaneous calcium transients was calculated by measuring the change in total pixel intensity for each normalized calcium transient trace. The rate was determined by dividing the total number of spontaneous calcium transients for any ROI by the total length of the movie (90 seconds). The synchronicity of spontaneous calcium transients was determined by two independent calculations. First, to determine the percentage synchronicity per calcium transient, the total number of synchronized calcium transients, defined as three or more simultaneous peaks, was divided by the total number of spontaneous calcium transients identified. Second, to calculate the maximum percentage synchronicity, the maximum number of ROIs involved in a single synchronized event was divided by the total number of ROIs identified.

CNV analysis

Cells were lysed in DNA Lysis solution (100 mM Tris, pH 8.5, 5 mM EDTA, 200 mM NaCl, 0.2% (w/v) sarcosyl, and 100 μg/ml fresh proteinase K) overnight at 50°C. DNA was precipitated by the addition of an equal volume of NaCl-ethanol mixture (150 μl of 5 M NaCl in 10 ml cold 95% ethanol) and then washed three times in 70% ethanol prior to resuspension in water with RNAseA overnight at 4°C.

Genome Scans were performed using NimbleGen HD2 arrays (NimbleGen Systems Inc) according the to the manufacturer's instructions using a standard reference genome SKN1. NimbleGen HD2 dual-color intensity data were normalized in a two-step process: first, a "spatial" normalization of probes was performed to adjust for regional differences in intensities across the surface of the array; second, the Cy5 and Cy3 intensities were adjusted to a fitting curve by invariant set normalization, preserving the variability in the data. The

$\log_2$ ratio for each probe was then estimated using the geometric mean of normalized and raw intensity data[25].

CNV analysis was completed to identify deletions and duplications present within our patients. By using a virtual "genotyping" step whereby individual CNV segment probe ratios were converted into z-scores, a distribution of median z-scores was generated, outliers of which were considered to be true CNVs. In doing so, we better filtered out common artifacts and false-positive CNVs and generated a list of CNVs unbiased by previous genetic studies of SCZD.

Patient fibroblasts were used for CNV analysis. Lymphocytes were available for patients 4 and 5 and their parents, allowing us to validate the CNVs identified for patient 4 and also to determine the parent of origin for each mutation; many were inherited from the unaffected mother (SI Table 7).

Gene expression analysis

Unless otherwise specified, gene expression analysis was performed on six-week-old hiPSC neurons without astrocyte coculture. Cells were lysed in RNA BEE (Tel-test, Inc). RNA was chloroform extracted, pelleted with isopropanol, washed with 70% ethanol and resuspended in water. RNA was treated with RQ1 RNAse-free DNAse (Promega) for 30 minutes at 37°C and then the reaction was inactivated by incubation with EGTA Stop buffer at 65°C for 10 minutes.

For gene expression microarrays, three independent neural differentiations for each of the four SCZD patients as well as four control subjects were compared using Affymetrix Human 1.0ST arrays as specified by the manufacturer.

Gene expression microarray analysis was completed using Partek Genomics Suite software. Intensity values were generated as follows: RMA background correction, quantile normalization, log2 transformation and mean polished probeset summarization. Pathway analysis was performed using Metacore GeneGo.

For qPCR, cDNA was synthesized using Superscript III at 50°C for one to two hours, inactivated for 15 minutes at 70°C and then treated with RNAaseH for 15 minutes at 37°C, inactivated with EDTA and heated to 70°C for 15 minutes. qPCR was performed using SybrGreen. Primers used are listed in SI Table 8.

Statistical analysis

Statistical analysis was performed using JMP (Carey, NC). Box-Cox transformation of raw data was performed to correct non-normal distribution of the data and residuals. Improvements were assessed by Shapiro-Wilk W test of the transformed data and residuals. Means were compared within diagnosis by Oneway analysis using both Student's T test and Tukey Kramer HSD. Finally, a nested analysis of values for individual patients was performed using standard least squares analysis comparing means for all pairs using Student's T test for specific pairs and Tukey Kramer HSD for multiple comparisons.

Supplementary Material

Refer to Web version on PubMed Central for supplementary material.

Acknowledgments

L. Moore, B. Miller, K. Stecker, J. Jepsen, D. Sepp, S. Larkin and L. Johnson provided technical assistance. T. Berggren directs, and M. Lutz manages, the Salk Stem Cell facility. D. Gibbs directs the Salk Viral Vector Core. J. Nguyen and L. Ouyang provided gene expression support. D. Chambers and J. Barrie provided FACS support. E. Callaway and I. Wickersham provided rabies trans-neuronal tracing viruses and invaluable advice and scientific feedback. M. Lawson provided incredible assistance with statistical analysis. Thanks to G. Yeo, M. McConnell, S. Aigner, C. Marchetto and L. Boyer for advice and conversation.

K.J.B. is supported by a training grant from the California Institute for Regenerative Medicine. The Gage Laboratory, and this project, is partially funded by CIRM Grant RL1-00649-1, The Lookout and Mathers Foundation, the Helmsley Foundation as well as Sanofi- Aventis.

ABBREVIATIONS

SCZD	schizophrenia
hiPSC	human induced pluripotent stem cell
NPC	neural progenitor cell
ENVA	envelope A
TVA	tumor virus A receptor
G	glycoprotein
H2BGFP	histone 2B green fluorescent protein fusion protein
GWAS	genome wide association study
SNP	single nucleotide polymo5phism
CNV	copy number variation
FACS	fluorescence activated cell sorter
GO	gene ontology

REFERENCES

1. Sullivan PF, Kendler KS, Neale MC. Schizophrenia as a complex trait: evidence from a meta-analysis of twin studies. Arch Gen Psychiatry. 2003; 60:1187–1192. [PubMed: 14662550]
2. Wong AH, Van Tol HH. Schizophrenia: from phenomenology to neurobiology. Neurosci Biobehav Rev. 2003; 27:269–306. [PubMed: 12788337]
3. Javitt DC, Spencer KM, Thaker GK, Winterer G, Hajos M. Neurophysiological biomarkers for drug development in schizophrenia. Nat Rev Drug Discov. 2008; 7:68–83. [PubMed: 18064038]
4. Ebert AD, et al. Induced pluripotent stem cells from a spinal muscular atrophy patient. Nature. 2009; 457:277–280. [PubMed: 19098894]
5. Lee G, et al. Modelling pathogenesis and treatment of familial dysautonomia using patient-specific iPSCs. Nature. 2009; 461:402–406. [PubMed: 19693009]
6. Marchetto MC, et al. A model for neural development and treatment of rett syndrome using human induced pluripotent stem cells. Cell. 2010; 143:527–539. [PubMed: 21074045]
7. Maherali N, et al. Directly Reprogrammed Fibroblasts Show Global Epigenetic Remodeling and Widespread Tissue Contribution. Cell Stem Cell. 2007; 1:55–70. [PubMed: 18371336]
8. Ugolini G. Use of rabies virus as a transneuronal tracer of neuronal connections: implications for the understanding of rabies pathogenesis. Dev Biol (Basel). 2008; 131:493–506. [PubMed: 18634512]
9. Wickersham IR, et al. Monosynaptic restriction of transsynaptic tracing from single, genetically targeted neurons. Neuron. 2007; 53:639–647. [PubMed: 17329205]
10. Lafon M. Rabies virus receptors. J Neurovirol. 2005; 11:82–87. [PubMed: 15804965]

11. Selemon LD, Goldman-Rakic PS. The reduced neuropil hypothesis: a circuit based model of schizophrenia. Biol Psychiatry. 1999; 45:17–25. [PubMed: 9894571]
12. Jaaro-Peled H, Ayhan Y, Pletnikov MV, Sawa A. Review of pathological hallmarks of schizophrenia: comparison of genetic models with patients and nongenetic models. Schizophr Bull. 2010; 36:301–313. [PubMed: 19903746]
13. Walsh T, et al. Rare structural variants disrupt multiple genes in neurodevelopmental pathways in schizophrenia. Science (New York, N.Y. 2008; 320:539–543.
14. Higgs BW, Elashoff M, Richman S, Barci B. An online database for brain disease research. BMC Genomics. 2006; 7:70. [PubMed: 16594998]
15. Patil ST, et al. Activation of mGlu2/3 receptors as a new approach to treat schizophrenia: a randomized Phase 2 clinical trial. Nat Med. 2007; 13:1102–1107. [PubMed: 17767166]
16. Patterson SL, et al. Some forms of cAMP-mediated long-lasting potentiation are associated with release of BDNF and nuclear translocation of phospho-MAP kinase. Neuron. 2001; 32:123–140. [PubMed: 11604144]
17. Freyberg Z, Ferrando SJ, Javitch JA. Roles of the Akt/GSK-3 and Wnt signaling pathways in schizophrenia and antipsychotic drug action. Am J Psychiatry. 2010; 167:388–396. [PubMed: 19917593]
18. Stefansson H, et al. Large recurrent microdeletions associated with schizophrenia. Nature. 2008; 455:232–236. [PubMed: 18668039]
19. Rare chromosomal deletions and duplications increase risk of schizophrenia. Nature. 2008; 455:237–241. [PubMed: 18668038]
20. Karayiorgou M, Gogos JA. The molecular genetics of the 22q11-associated schizophrenia. Brain Res Mol Brain Res. 2004; 132:95–104. [PubMed: 15582150]
21. Wang XD, Su YA, Guo CM, Yang Y, Si TM. Chronic antipsychotic drug administration alters the expression of neuregulin 1beta, ErbB2, ErbB3, and ErbB4 in the rat prefrontal cortex and hippocampus. Int J Neuropsychopharmacol. 2008; 11:553–561. [PubMed: 18184445]
22. Kapur S, et al. PET evidence that Loxapine is an equipotent blocker of 5-HT2 and D2 receptors: implications for the therapeutics of schizophrenia. Am J Psychiatry. 1997; 154:1525–1529. [PubMed: 9356559]
23. Cannon TD, Keller MC. Endophenotypes in the genetic analyses of mental disorders. Annu Rev Clin Psychol. 2006; 2:267–290. [PubMed: 17716071]

SI REFERENCES

24. Association, A. P.. Diagnostic and statistical manual of mental disorders: DSM-IV. 3rd ed., rev. edn, Vol. 4th ed. American Psychiatric Press; 1994.
25. McCarthy SE, et al. Microduplications of 16p11.2 are associated with schizophrenia. Nature genetics. 2009; 41:1223–1227. [PubMed: 19855392]

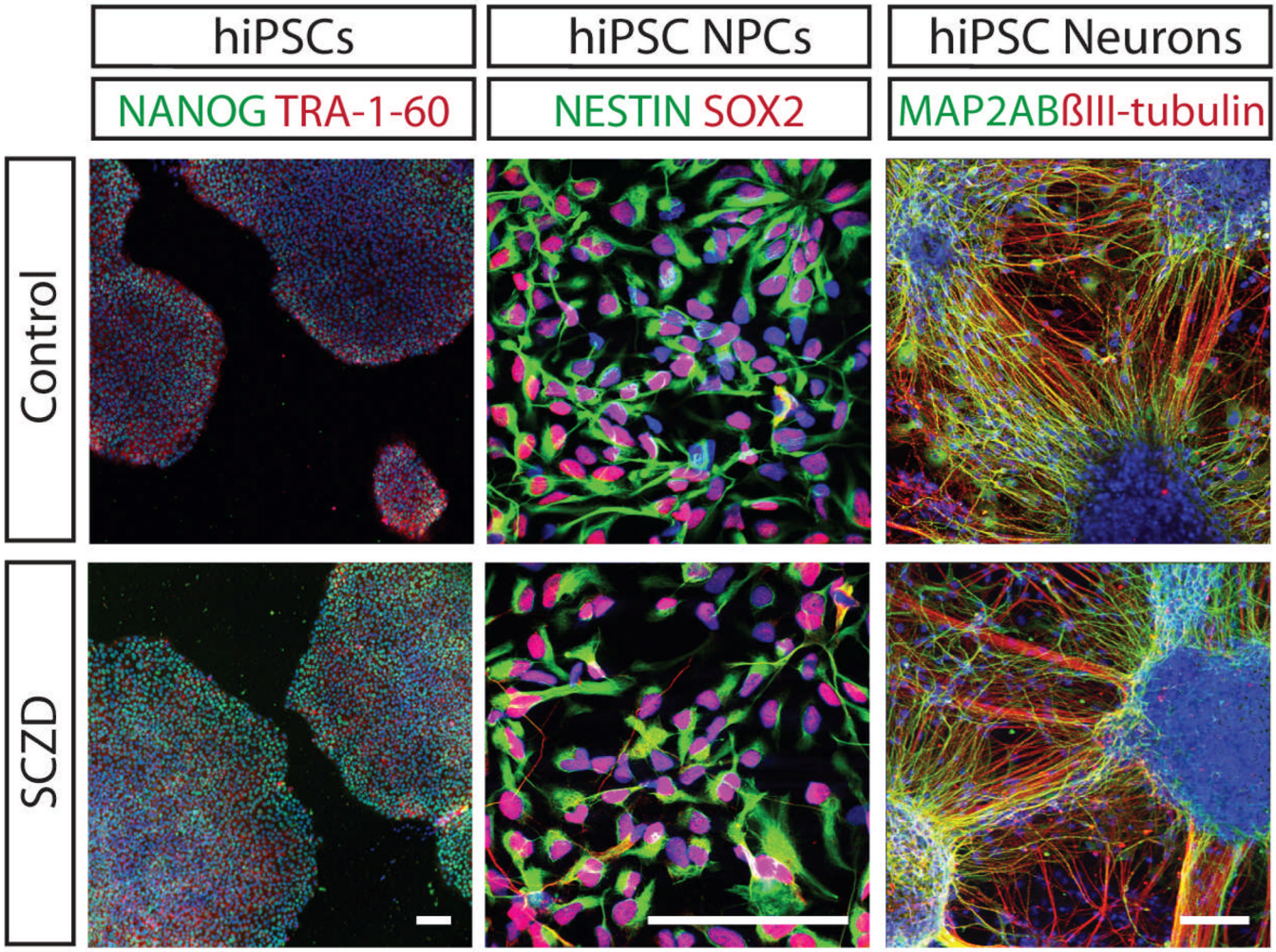

Fig. 1. Patient-specific hiPSCs, NPCs and neurons

Left. hiPSCs express NANOG (green) and TRA-1-60 (red). DAPI (blue). ×100, scale bar 100 μm. **Centre**. hiPSC neural progenitor cells (NPCs) express NESTIN (green) and SOX2 (red). DAPI (blue). ×600, scale bar 100 μm. **Right**. hiPSC neurons express βIII-tubulin (red) and the dendritic marker MAP2AB (green). DAPI (blue). ×200, scale bar 100 μm.

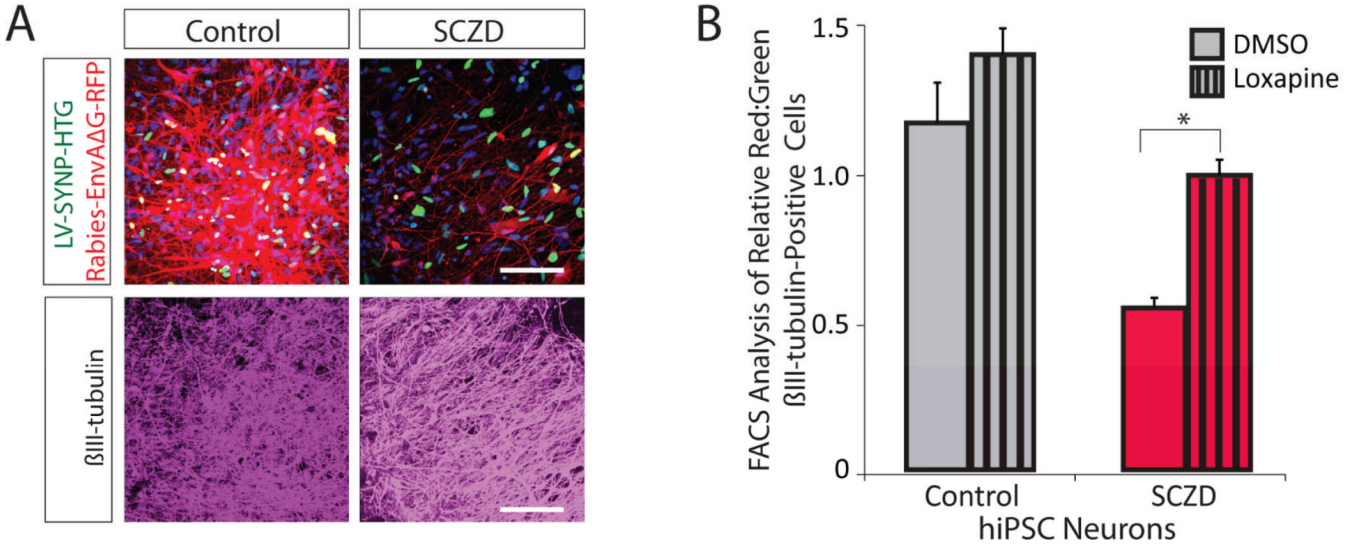

Fig. 2. Decreased neuronal connectivity in SCZD hiPSC neurons

A. Representative images of control and SCZD hiPSC neurons cotransduced with LV-SYNP-HTG and Rabies-ENVAΔG-RFP, 10 days post rabies transduction. All images were captured using identical laser power and gain settings. βIII-tubulin staining (purple) of the field is shown below each panel. ×400, scale bar 80 μm. **B**. Graph showing treatment of SCZD hiPSC neurons with Loxapine resulted in a statistically significant improvement in neuronal connectivity. Error bars are s.e., *P < 0.05.

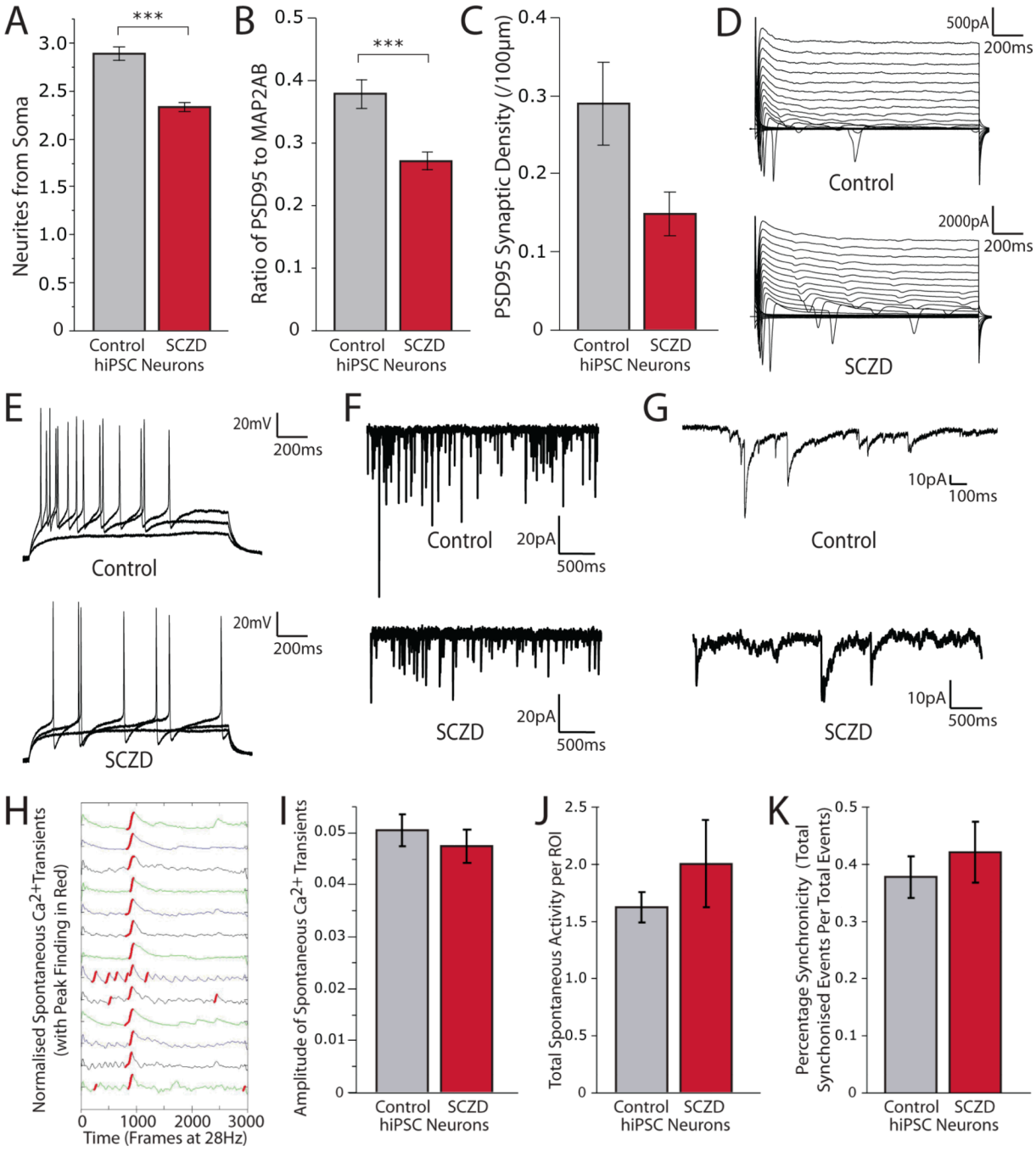

Fig. 3. Decreased neurites and synaptic protein levels but normal electrophysiological and spontaneous calcium transient activity in SCZD hiPSC neurons

A. Graph showing decreased neurites in SCZD hiPSC neurons. **B.** Graph showing decreased PSD95 protein relative to MAP2AB for SCZD hiPSC neurons. **C**. Graph showing a trend of decreased PSD95 synaptic density in SCZD hiPSC neurons. **D–G.** Electrophysiological characterization. hiPSC neurons cultured on astrocytes show normal sodium and potassium currents when voltage-clamped **(D),** normal induced action potentials when current-clamped **(E)**, and spontaneous excitatory **(F)** and inhibitory **(G)** synaptic activity. **H–K**. Spontaneous calcium transient imaging. Representative spontaneous Fluo-4AM calcium traces of fluorescent intensity versus time generated from three-month-old hiPSC neurons **(H).** Graph

showing no difference between the spike amplitude of spontaneous calcium transients of control and SCZD hiPSC neurons **(I).** Graph showing no difference between the total numbers of spontaneous calcium transients per total number of ROIs in cultures of control and SCZD hiPSC neurons **(J).** Graph showing no change in percentage synchronicity per calcium transient in control and SCZD hiPSC neurons **(K).** Error bars are SE. Asterisks used as follows: *** $p<0.001$.

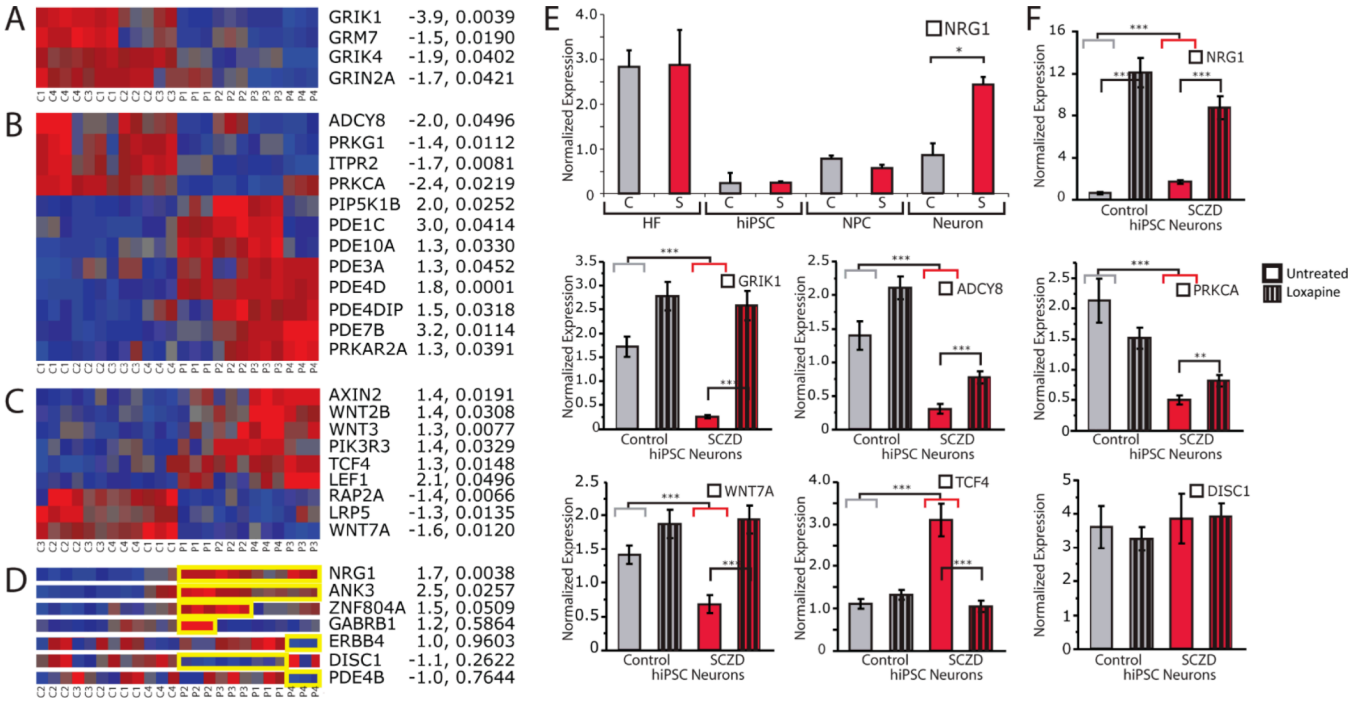

Fig. 4. RNA expression analysis of control and SCZD hiPSC neurons

A–C. Heat maps showing microarray expression profiles of altered expression of glutamate receptors **(A),** cAMP signaling **(B),** and WNT signaling **(C)** genes in SCZD hiPSC neurons. Fold-change and p-values (diagnosis) provided to the right of each heat map. **D.** Heat maps showing perturbed expression (highlighted in yellow) of NRG1 and ANK3 in all four SCZD patients, as well as altered expression of ZNF804A, GABRB1, ERBB4, DISC1 and PDE4B in some but not all patients. Fold-change and p-values (diagnosis) provided to the right of each heat map. **E.** Altered expression of NRG1 is detected in SCZD hiPSC neurons but not in patient fibroblasts, hiPSCs or hiPSC NPCs. **F.** qPCR validation of altered expression of NRG1, GRIK1, ADCY8, PRKCA, WNT7A, TCF4 and DISC1, as well as response to three weeks of treatment with Loxapine (striped bars) in six-week-old hiPSC neurons. Asterisks used as follows: * $p<0.05$, ** $p<0.01$, *** $p<0.001$.